Available online at www.sciencedirect.com
SCIENCE DIRECT®
Tetrahedron: Asymmetry
Tetrahedron: *Asymmetry* 16 (2005) 1035–1046

5-Thio-D-glycopyranosylamines and their amidinium salts as potential transition-state mimics of glycosyl hydrolases: synthesis, enzyme inhibitory activities, X-ray crystallography, and molecular modeling

Lizie M. Kavlekar,[a] Douglas A. Kuntz,[b] Xin Wen,[a] Blair D. Johnston,[a] Birte Svensson,[c,†] David R. Rose[b,*] and B. Mario Pinto[a,*]

[a]*Department of Chemistry, Simon Fraser University, Burnaby, British Columbia, Canada V5A 1S6*
[b]*Ontario Cancer Institute and Department of Medical Biophysics, University of Toronto, 610 University Avenue, Toronto, Ontario, Canada M5G 2M9*
[c]*Department of Chemistry, Carlsberg Laboratory, Gamle Carlsberg Vej 10, DK-2500 Valby, Denmark*

Received 9 December 2004; revised 21 December 2004; accepted 5 January 2005

Abstract—The synthesis of new glycosidase inhibitors, namely, the glycosylamines of 5-thioglucose and 5-thiomannose and their corresponding amidinium salts are described. We report also the crystal structures of 5-thio-D-mannopyranosyl amine **1** and 5-thio-D-mannopyranosylamidinium bromide **2** bound in the enzyme active site of Golgi α-mannosidase II (GM II). Compounds **1** and **2** have been found to be inhibitors with IC_{50} values of 0.07 and 0.9 mM, respectively. We also report the docked structures of 5-thio-D-glucopyranosylamine **3** and 5-thio-D-glucopyranosylamidinium bromide **4** in the active site of glucoamylase G2, derived by molecular modeling. Compounds **3** and **4** were found to be inhibitors with K_i values of 0.015 and 0.098 mM, respectively. The results led to conclusions about the nature of the transition state and strategy for the inhibition of glycosyl hydrolases in general.
© 2005 Elsevier Ltd. All rights reserved.

1. Introduction

Glycosidases are involved in the processing of various glycoconjugates, such as glycoproteins, which in turn are involved in various biological processes.[1] These glycoproteins are formed via a common glycolipid precursor, Glc_3-Man_9-$GlcNAc_2$-pyrophosphoryl-dolichol, which in turn is formed by the dolichol pathway.[1,2] This precursor is transferred to the asparagine residues of proteins in the endoplasmic reticulum (ER) by an oligosaccharyl transferase enzyme. Carbohydrate units attached to asparagine residues have a common inner-core structure. Subsequent trimming and processing of this precursor in the ER and the Golgi apparatus, carried out by glycosidases and glycosyltransferases, leads to a variety of *N*-linked glycans targeted to perform particular biological functions. The functioning of these glycoproteins will depend on the exact nature of the attached oligosaccharides. The surface oligosaccharides mediate a variety of biological phenomena including cell–cell or cell–virus recognition processes. Inhibition of glycosidases can disrupt the biosynthesis of oligosaccharides and hence influence such processes as cancer cell metastasis. Thus, the design, synthesis, and X-ray crystallographic and molecular modeling studies of their inhibitors have become interesting research areas for the design of new drugs.

Herein, we report a class of inhibitors based on 5-thio-D-glycopyranosylamines (Chart 1). Glycosylamines themselves can act as glycosidase inhibitors,[3] although they hydrolyze readily. We reasoned that since the S/N acetals are more stable to hydrolysis,[4,5] compounds **1** and **3** and the corresponding glycosylamidinium salts **2** and **4** might offer advantages over their oxygen congeners.

* Corresponding authors. Tel.: +1 416 946 2970; fax: +1 416 946 6529 (D.R.R.); tel.: +1 604 291 4327; fax: +1 604 291 5424 (B.M.P.); e-mail addresses: drose@oci.utoronto.ca; bpinto@sfu.ca
† Present address: Biochemistry and Nutrition Group, BioCentrum-DTU, Denmark Technical University, Søltofts Plads Bldn 224, DK-2800 Kgs. Lyngby, Denmark.

0957-4166/$ - see front matter © 2005 Elsevier Ltd. All rights reserved.
doi:10.1016/j.tetasy.2005.01.021

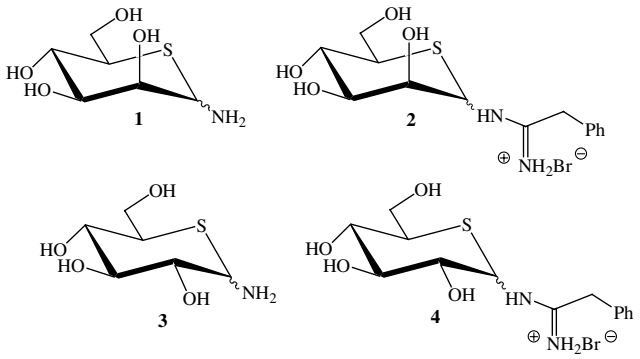

Chart 1.

Glycosylamidinium salts themselves have been shown to have inhibitory properties,[6] and have been used as ligands for affinity chromatography for β-glycosidases.[7] We also report the interactions of inhibitors **1**–**4** with two glycosyl hydrolases of different families, three-dimensional structures, and catalytic mechanism. As the transition states of the retaining and inverting glycosidase mechanisms share many structural and chemical characteristics, a comparison of compounds, which can act as transition-state mimics for both mechanisms, would reveal conclusions concerning general strategies for inhibiting glycosyl hydrolases.

Golgi α-mannosidase II (GMII) is a key enzyme involved in *N*-glycan processing.[1,2] Inhibitors that target GMII have been shown to act as potential anticancer agents.[8] GMII belongs to the glycosyl hydrolase family 38. It specifically trims two mannose residues from the branched $GlcNAcMan_5GlcNAc_2$ mannose intermediate during *N*-glycan processing. The hydrolysis of the glycosidic bonds takes place with retention of configuration at the anomeric center.[9] We report herein that glycosylamine **1** and the corresponding amidinium salt **2** inhibit *Drosophila* GMII with IC_{50} values of 0.07 and 0.9 mM, respectively. We report also the X-ray crystallographic analysis of the complexes of **1** and **2** with GMII, which has provided insight into the requirements of potential transition-state mimics.

Glucoamylase G2 is an *exo*-acting inverting glycosidase of Family 15 that catalyzes the release of β-D-glucose from the nonreducing ends of starch and related polysaccharides and oligosaccharides.[10] Glycosylamine **3** and the corresponding amidinium salt **4** were found to be inhibitors of glucoamylase G2, with K_i values of 0.098 and 0.015 mM, respectively. In the absence of X-ray crystal structures of complexes of **3** and **4** with glucoamylase G2, we present herein molecular modeling studies of the complexes from which we infer the requirements for transition-state mimics.

2. Results and discussion

2.1. Synthesis

Consideration of the structures of the amidinium salts **2** and **4** shows that they can be synthesized by the coupling reaction of 5-thio-D-glycopyranosylamines **1** and **3** with a thioimidate salt **5**, in an analogous fashion to that reported for the preparation of the corresponding glycopyranosylimidates.[11] The glycosylamines can be synthesized in turn from the 5-thio-D-glycopyranoses (Scheme 1). 5-Thio-D-mannose **6** and 5-thio-D-glucose **7** were synthesized using literature procedures.[12,13]

The reaction of 5-thio-D-glucose **7** in methanol saturated with ammonia gave an α:β (1:2) mixture of the 5-thio-D-glucosylamines **3** in low yield (2–15%). Addition of potassium carbonate, variation of the reaction temperatures from room temperature to 70 °C, or alteration of the reaction duration did not result in significant improvement in yield, the reactions also yielded many side products. All these attempts gave the desired product in very low yield. During the above attempts, it was observed that the product decomposed above 50 °C and that higher yields were obtained for reactions carried out at room temperature. The reaction of **7** in aqueous ammonia at rt for 3 days proved more promising and gave the desired glucosylamines **3** as an α:β (1:2) mixture in 76% yield (Scheme 1). The α- and β-configurations were assigned based on the H1–H2 coupling constants. A similar procedure starting with 5-thio-D-mannose **6** yielded the 5-thio-D-mannopyranosylamines **1** as an α:β (1:3) mixture in 77% yield (Scheme 1). The α- and β-isomers were assigned based on NOE experiments.

The synthesis of the corresponding 5-thio-D-glucosylimidates **4** was then examined. Reaction of thioimidate salt **5**[6] with 5-thio-D-glucopyranosylamines **3** in pyridine gave a mixture of five compounds, as indicated by ^1H NMR spectroscopy. The desired compounds **4** were obtained as an α:β (1:7) mixture in 30–35% yield. In all these reactions, the starting material was not totally consumed and could be recovered. A sample enriched in the β-isomer (α:β 1:15) was obtained after HPLC purification.

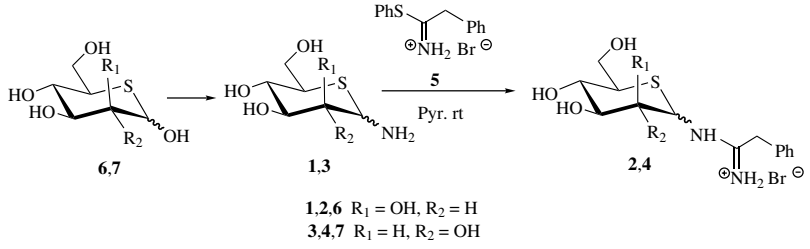

Scheme 1.

The 5-thio-D-mannopyranosylimidates **2** were obtained as an α:β (1:3) mixture in 37% yield using the same procedure. As before, the reaction did not proceed to completion and the starting material could be recovered. In this case, HPLC purification yielded separate α- and β-isomers. The α- and β-configurations were assigned based on NOE experiments. Thus, the NOESY spectra for compounds **6α** did not show any cross peaks for H-1/H-3 and H-1/H-5, confirming the α-configuration, while compound **6β** showed cross peaks for H-1/H-3 and H-1/H-5 and was assigned to be the β-isomer.

2.2. Enzyme inhibition

Compounds **1** and **2** were found to inhibit Golgi α-mannosidase II with inhibition constants IC_{50} of 7.0×10^{-2} and 9.0×10^{-1} mM, respectively. Compounds **3** and **4** inhibited maltose hydrolysis by glucoamylase G2[14,15] with K_i values 9.8×10^{-2} and 1.5×10^{-2} mM, respectively.

2.3. X-ray crystallography

X-ray crystal structures of compounds **1** and **2** (Fig. 1) bound in the active site of the *Drosophila* GMII orthologue indicated that both compounds were each bound as the α-anomer. Compound **1** (Figs. 1 and 2) adopted a strained boat conformation (^{1,4}B) stabilized by electrostatic interactions and hydrogen bonding in the enzyme active site. The positively charged nitrogen atom in **1** has electrostatic interactions with Tyr A269 and Asp A341(OD2) (Fig. 2, Table 1). The hydroxyl groups 2-OH, 3-OH, and 6-OH form hydrogen bonds with Asp A92 (OD2), Asp A472 (OD2), and Arg A876, respectively. The 4-OH group forms hydrogen bonds with Asp A472 (OD1) and Tyr A727 (Fig. 2, Table 1).

Compound **2** is also found to bind in a boat conformation (^{1,4}B) and shows similar hydrogen bonding interactions as in compound **1** with the enzyme active site (Figs. 1 and 2; Table 1). The anomeric nitrogen atom in compound **2** is probably protonated in the enzyme active site and shows an electrostatic interaction with Asp A341 (OD2). The hydroxyl groups 2-OH, 3-OH, and 6-OH, are hydrogen bonded to Asp A92 (OD2), Asp A472 (OD2), and Arg A876, respectively, as in compound **1**. The 4-OH group forms hydrogen bonds with Asp A472 (OD1) and Tyr A727, as with compound **1**. The 6-OH group is hydrogen bonded to a water molecule.

In order to explain the difference in the inhibition constants for compounds **1** and **2**, the crystal structures of both complexes were compared (Fig. 2). The corresponding OH groups in both compounds form hydrogen bonds with the same amino acids in the enzyme active site. The significant difference is the additional charged hydrogen bond between the positively charged nitrogen atom at the anomeric center in compound **1** and Tyr A269. This interaction probably contributes to the increased binding affinity of compound **1** to GMII.

Both compounds **1** and **2** are further stabilized by the coordination of the O2 and O3 hydroxyl oxygens to zinc. As described previously,[9] for the case of the complex of GMII with the known glycosidase inhibitor, swainsonine **8**, zinc is found to adopt a T_6 geometry (octahedral coordination) involving four amino acid residues, His 90, Asp 92, His 471, Asp 204, and the O2 and O3 hydroxyl oxygens (Fig. 3). We have proposed that this octahedral coordination aids in the distortion of the six-membered ring to mimic the transition state in the glycosidase-mediated hydrolysis reaction.[16]

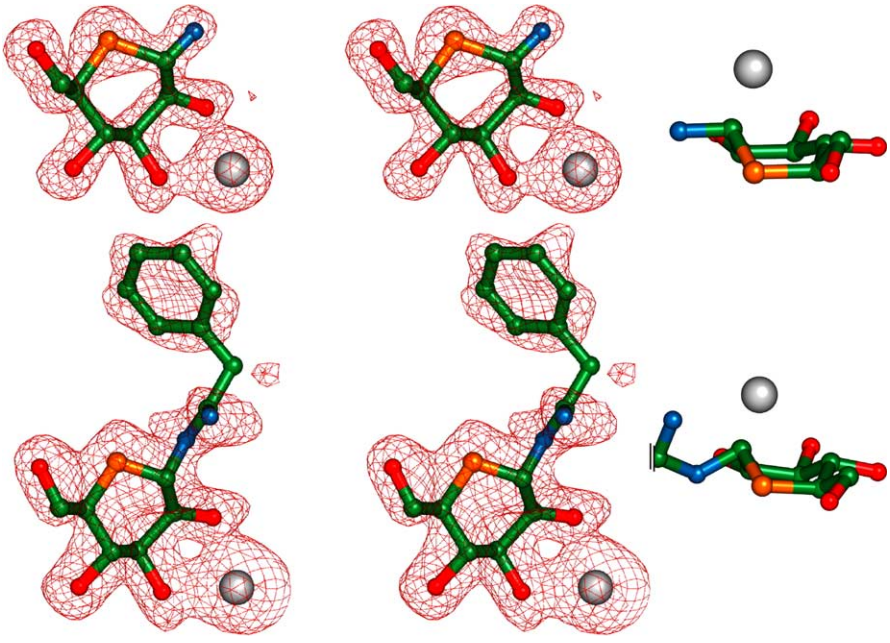

Figure 1. Electron density of compounds **1** and **2** bound in the active site of dGMII. Simulated annealing omit maps (1Fo–Fc) contoured at 4.0 sigma for compound **1** (top) and 2.0 sigma for compound **2** (bottom). The boat conformation of the six-membered rings of each of the compounds is shown on the right. The figure was generated using Pymol.[30]

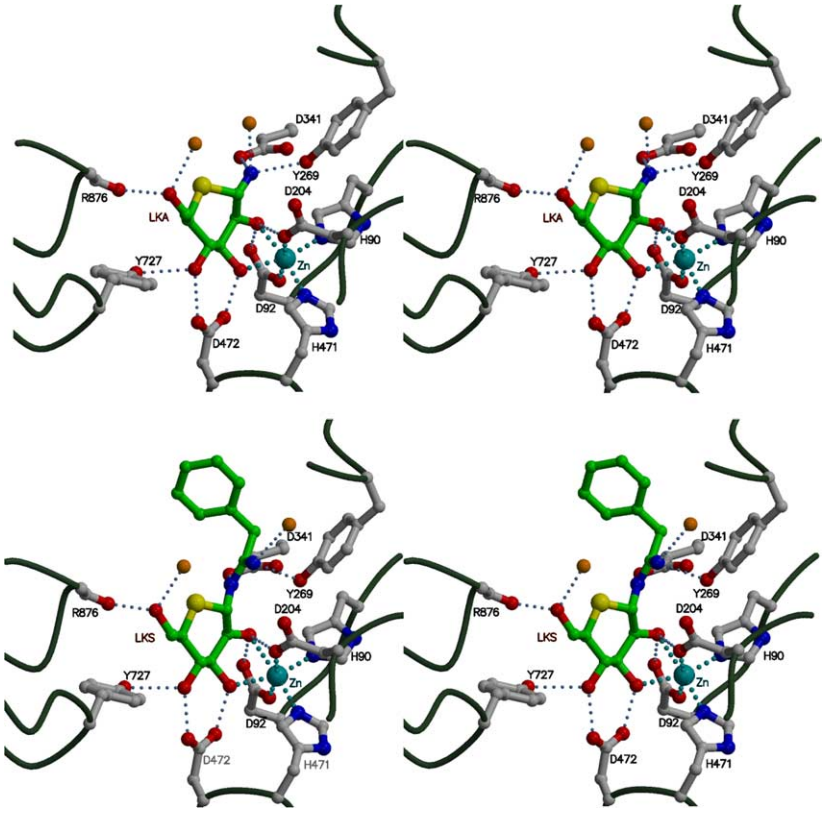

Figure 2. Stereoview of the interactions of **1** (top) and **2** (bottom) with the active site of dGMII. Interactions closer than 3.5 Å are indicated in blue. The interactions with the zinc ion are indicated in cyan. Interacting water molecules appear as orange balls. The distances are presented in Table 2. This figure was generated with the program Molscript.[31]

Table 1. Distances between interacting atoms in dGMII complexes of **1**, **2**, and **8**

dGMII in complex with:		**8** Swainsonine		**1** LKA	**2** LKS
Zinc interactions					
Protein Atom		Distance (Å)	Inhibitor atom	Distance (Å)	Distance (Å)
H90 NE2		2.14		2.14	2.11
D92 OD1		2.16		2.21	2.15
D204 OD1		2.16		2.16	2.24
H471 NE2		2.16		2.14	2.17
Inhibitor interactions					
Protein atom	Inhibitor atom				
Zn	OH-1	2.31	OH-3	2.22	2.30
	OH-2	2.30	OH-2	2.23	2.28
D92 OD1	OH-1	3.08	OH-3	3.04	2.95
	OH-2	2.91	OH-2	3.07	3.12
D92 OD2	OH-2	2.43	OH-2	2.50	2.32
D204 OD1	OH-1	2.83	OH-2	3.03	3.14
	N	2.88	S^+	4.53	4.44
D204 OD2	N	3.55	S^+	4.72	4.58
Y269 OH	—	—	N2	2.69	2.93
D341 OD2	—	—	N1	2.92	2.84
D472 OD1	OH-8	2.51	OH-4	2.70	2.62
D472 OD2	OH-1	2.61	OH-3	2.55	2.52
Y727 OH	OH-8	2.69	OH-4	2.78	2.81
R876 O	—	—	OH-6	2.68	2.53
Waters			OH-6	2.71	2.62
			N1[a]	2.72	—
			N2[b]	—	3.07

[a] N1 refers to the anomeric nitrogen atom.
[b] N2 refers to the nonanomeric nitrogen atom.

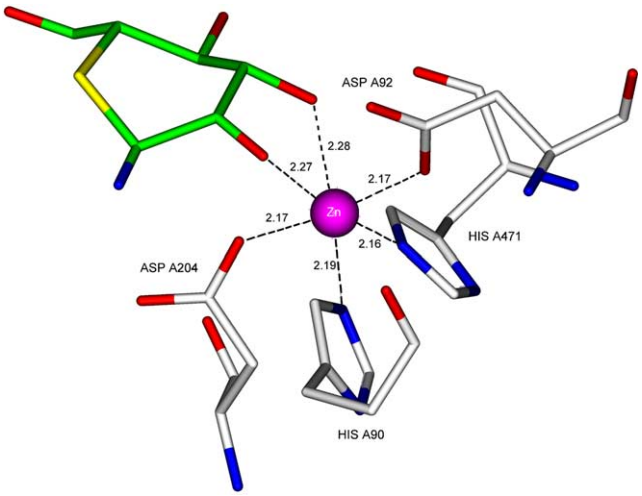

Figure 3. Interaction of compound **1** with Zn in the enzyme active site of GM II.

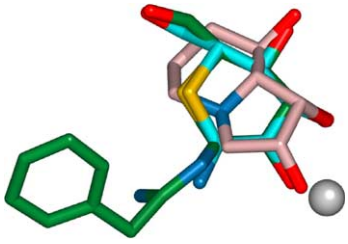

Figure 4. Overlay of swainsonine **8** with compounds **1** and **2**. **1** cyan, **2** green, **8** pink.

It is worthwhile comparing the crystal structures of compounds **1**, **2**, and swainsonine **8**, a nanomolar inhibitor of *Drosophila* GMII,[9] in the enzyme active site (Fig. 4, Chart 2). The 2-OH and 3-OH groups of **8** form hydrogen bonds with Asp A92 (OD1 and OD2), Asp A204, and Asp A472. This causes the inhibitor molecule to tilt in an orientation relative to the other compounds. The tilting facilitates the electrostatic attraction of the protonated nitrogen with Asp A204 (OD1) (with a hydrogen bond length of 2.88 Å). Conversely, in compounds **1** and **2** there is no significant interaction with Asp A204 [(N1–Asp A204 = 3.69 Å (OD1), 3.92 Å (OD2), N1–Asp A204 = 4.23 Å (OD1), 4.59 Å (OD2), respectively)] (Fig. 4). The positively charged nitrogen atom in **1** does show a strong interaction with Tyr 269 and Asp 341. Similarly, in compound **2** the positively charged center interacts with Asp 341.

A detailed comparison of the amidinium salt **2** and swainsonine **8** bound in the active site of GMII is shown in Figure 5. The amino acids with the greatest range of motion between the two complexes are Y269 and R228, with movements of 0.89 and 1.03 Å, respectively.

2.4. Molecular modeling

Due to the X-ray crystal structures of **3** and **4** complexed to glucoamylase G2 not being available, molecular modeling studies were performed to investigate the interactions of the corresponding inhibitors **3** and **4** in the active site; the starting point for these studies was the enzyme structure complexed with deoxynojirimycin **9**.[17]

Molecular modeling with the program AutoDock 3.0 was used to generate various docked structures of **3** and **4** in the glucoamylase G2 active site, and the probable conformations of bound **3** and **4** were obtained by selecting structures with the lowest binding energy.

Compound **3** binds in the half chair ($^2H_3$) conformation (Fig. 6). The important interactions of compound **3** with residues in the enzyme active site are listed in Table 2.

As seen in Figure 6, the 3-OH group shows hydrogen bonding interactions with Arg 54 and Leu 177, the 4-OH group shows hydrogen bonding with Arg 54 and Asp 55, and the 6-OH group shows hydrogen bonding with Asp 55 and a water molecule. The positively charged nitrogen atom in **3** interacts with Trp 178 and Glu 179.

Compound **4** also binds in a half chair ($^2H_3$) conformation (Fig. 7). The interactions with the amino acid residues in the active site of glucoamylase G2 are listed in Table 2. The 3-OH group forms hydrogen bonds with Arg 54 and the carbonyl group of Leu 177. The 4-OH group shows hydrogen bonding with Asp 55 and Arg 54, and the 6-OH group shows hydrogen bonding with Asp 55 and a water molecule. The positively charged anomeric nitrogen atom in **4** interacts with Glu 179, and the nonanomeric nitrogen atom with Tyr 48 and Tyr 311 (Fig. 7). Comparison of the interactions of compounds **3** and **4** in the active site indicates that the only significant difference is the close contact between the

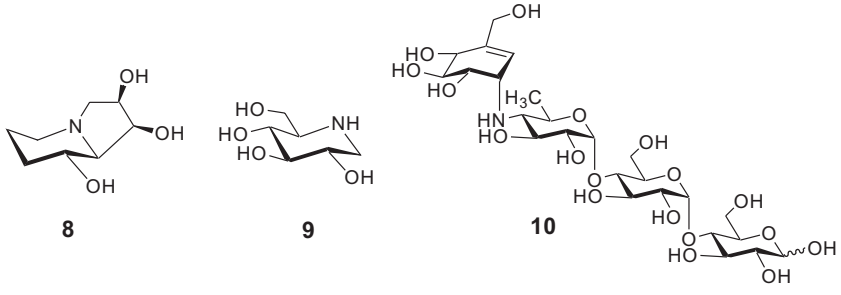

Chart 2.

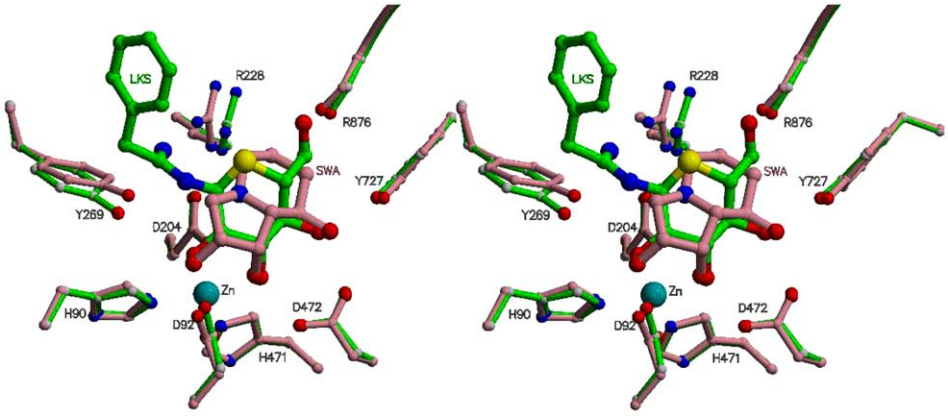

Figure 5. Comparison of the binding of compound **2** and swainsonine **8** in the active site of dGMII. Compound **2** and its interacting amino acids are indicated in green. Swainsonine **8** and interactions with the comparable amino acids are indicated in pink.

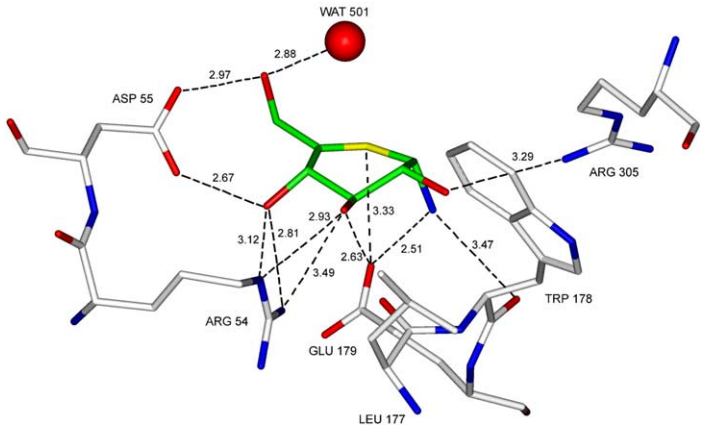

Figure 6. Compound **3** modeled in the active site of glucoamylase G2.

Table 2. Interactions of polar groups of compounds **3**, **4**, **9**, and **10** with residues in the active site of glucoamylase G2

Groups	Amino acids of glucoamylase G2	Distance (Å)			
		Compound **3**	Compound **4**	Compound **9**[a]	Compound **10**[b,c]
OH-2	ARG 305:NH1	3.29	3.49	3.23	2.99
OH-3	ARG 54:NE	2.93	2.77	3.27	3.39
	ARG 54:NH2	3.49	3.06		
	LEU 177:O	2.63	2.61	2.65	2.73
OH-4	TRP 52: NE1		3.36		
	ARG 54:NE	3.12	3.43	3.32	3.12
	ARG 54:NH2	2.81	2.89	2.91	2.86
	ASP 55:OD1	2.67	2.67	2.73	2.80
OH-6	ASP 55:OD2	2.97	2.80	2.57	2.77
	WAT 501	2.88	2.97		
N1	TRP 178:O	3.47			
	GLU 179:OE2	2.51	2.92[d]		2.66
	WAT 501			2.82	
	WAT 634			2.82	
N2[e]	TYR 48:OH		2.49		
	TYR 311:OH		3.00		

[a] From the crystal structure of the complex.[17]
[b] From the crystal structure of the complex.[18]
[c] OH-2, OH-3, OH-4, and OH-6 refer to the A ring.
[d] N1 refers to the anomeric nitrogen atom.
[e] N2 refers to the nonanomeric nitrogen atom.

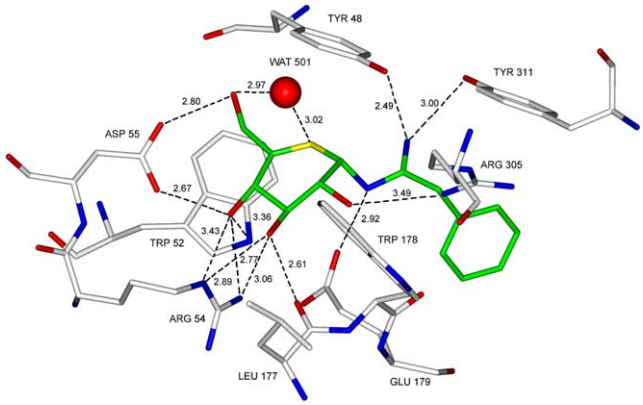

Figure 7. Compound **4** modeled in the active site of glucoamylase G2.

nonanomeric nitrogen atom in **4** with Tyr 48 and Tyr 311. This difference is presumably responsible for the increased binding affinity of compound **4** to glucoamylase G2.

The modeled structures of compounds **3** and **4** were then compared to that of 1-deoxynojirimycin **9**, a nanomolar inhibitor of glucoamylase G2, bound in the active site (see Figs. 8 and 9).[17] The interactions of **9** with glucoamylase G2 are listed in Table 2. Comparison of the structures is based on the dominant interaction of the positively charged center with the active site amino acids of glucoamylase G2. The positive center in 1-deoxynojirimycin **9** interacts with two water molecules Wat 634 and Wat 501. The hydrogen bond with W 501 in turn interacts with Glu 400. In compound **3**, on the other hand, the positively charged center interacts with Glu 179 (Fig. 8). The positive center in **4** interacts with Tyr 48 (OH) and Tyr 311 (Fig. 9). The 2-OH, 3-OH, 4-OH, and 6-OH groups in compounds **3** and **4** share similar interactions with **9** in the enzyme active site.

It was also noteworthy to compare the modeled complexes of glucoamylase G2 with **3** and **4** to that of the crystallographically-determined structure of the gluco-

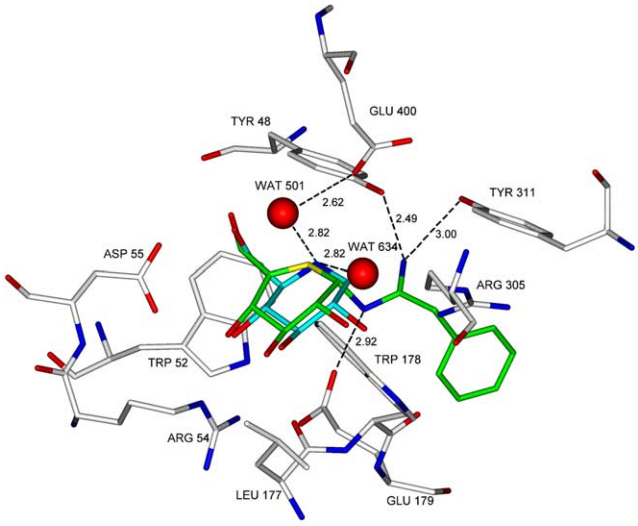

Figure 9. Superimposition of compound **4** with compound **9** in the active site of glucoamylase G2.

amylase G2–acarbose **10** complex;[18] acarbose **10** is a known glycosidase inhibitor. It is clear from Figures 10 and 11 that ring A of acarbose **10** superimposes well on the half-chair conformation of the six-membered ring in compounds **3** and **4**, the positively charged anomeric nitrogen atom interacting with Glu 179 in all three cases.

2.5. Ring distortion

Of special note is the ring distortion displayed by the inhibitors **1**–**4** when bound in the active sites of the respective enzymes. The widely held belief is that the transition state in a glycosidase-catalyzed hydrolysis reaction is one in which the six-membered ring is distorted to a half chair conformation. Accordingly design efforts for new inhibitors have focused on mimicking the half chair conformation, although there are some reports of mimicking a boat conformation.[19] The possibility of a boat transition state has gained some support from the reported crystal structure of cellobiohydrolase

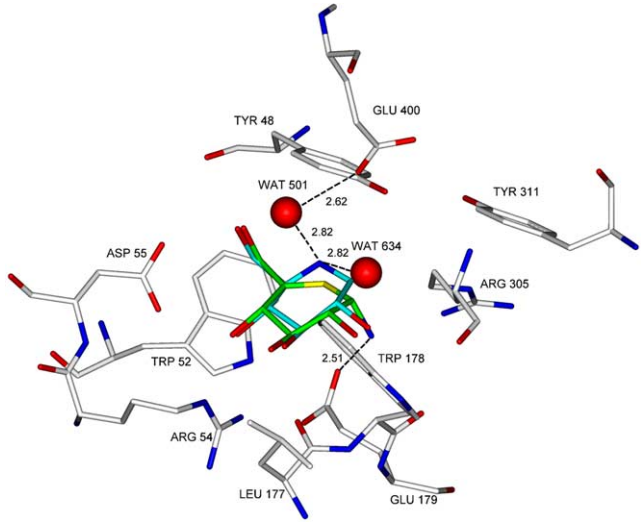

Figure 8. Superimposition of compound **3** with compound **9** in the active site of glucoamylase G2.

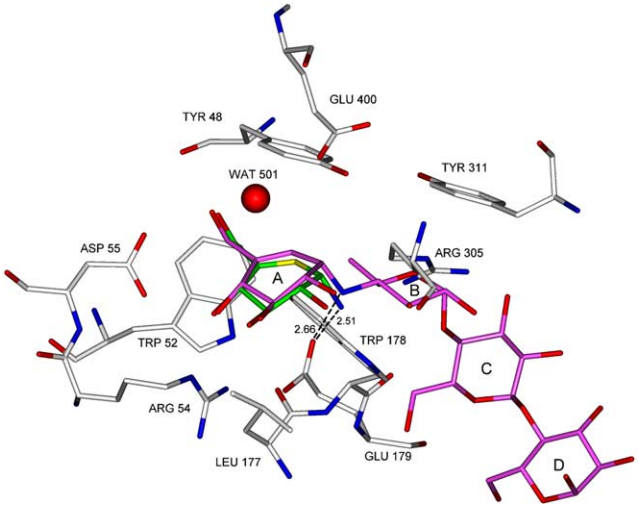

Figure 10. Superimposition of compound **3** with compound **10** in the active site of glucoamylase G2.

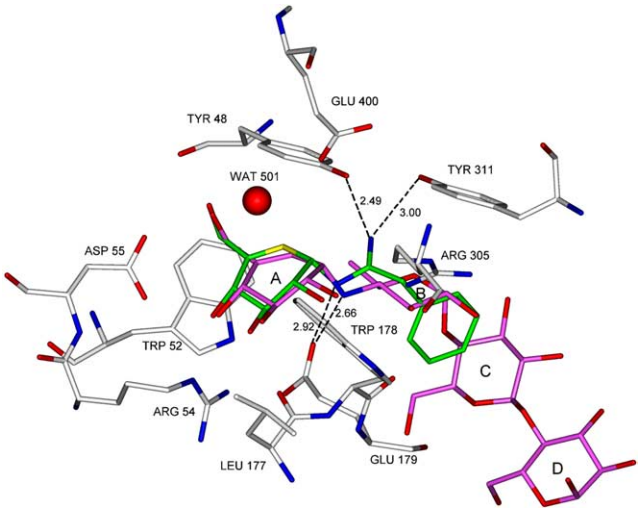

Figure 11. Superimposition of compound **4** with compound **10** in the active site of glucoamylase G2.

CelA, in complex with cellohexaose **11** (Chart 3).[20] The glucosyl residue D is bound in the active site in a distorted $^{2,5}B$ conformation, which presumably facilitates the formation of an oxacarbenium ion intermediate and cleavage of the D–C glycosidic bond. Vaarot et al.[21] have also reported a $^{2,5}B$ conformation for the isofagomine ring of **12** in the active site of the inverting β-glucosidase Cel6A. A similar observation of a $^{2,5}B$ conformation of manno-noeuromycin **13** in the active site of GMII has been noted.[22] In this regard, it is also relevant that the structure of a covalent GMII-linked intermediate derived from the inhibitor 5-fluoro-β-L-gulopyranosyl fluoride (5FGulF) **14** indicates that the ring adopts an $^{1}S_5$ conformation with Asp 204 attached to the anomeric carbon.[23] Finally, Johnson et al. have reported that the sulfonium-ion glycosidase inhibitor **15** is bound by glucoamylase G2 in a conformation in which the six-membered ring adopts a high-energy boat ($^{1,4}B$) conformation.[24]

3. Conclusions

X-ray crystallographic studies indicate that compounds **1** and **2** adopt a boat ($^{1,4}B$) conformation when bound in the active site of Golgi α-mannosidase II. Molecular modeling studies suggest that compounds **3** and **4** adopt a boat ($B_{1,4}$) and half chair conformation ($^{2}H_3$), respectively, when bound in the active site of glucoamylase G2. The strained conformations are stabilized by the various hydrogen bonds and electrostatic interaction between the protonated nitrogen atom and a carboxylate group or a tyrosine residue in the enzyme active site. Since compounds **1**–**4** exhibit distorted ring conformations and charged interactions within the enzyme active sites, it is likely that they function as transition-state analogues. It is interesting that these inhibitors have similar binding properties, specifically strained ring conformations, in two structurally unrelated families of glycosyl hydrolases operating by different catalytic mechanisms. This emphasizes the similarities of the nature of the transition states of inverting and retaining glycosidases. Finally, this class of compound may represent a general starting point for the design of inhibitors of many glycosyl hydrolases.

4. Experimental

4.1. General

Optical rotations were measured with a Rudolph Research Autopol II automatic polarimeter. ^{1}H NMR and ^{13}C NMR spectra were recorded on a Bruker AMX-400 NMR spectrometer at 400.13 and 100.6 MHz, for ^{1}H and ^{13}C, respectively. Chemical shifts are given in ppm downfield from TMS for those spectra measured in $CDCl_3$ or CD_3OD and from 2,2-dimethyl-2-silapentane-5-sulfonate (DSS) for those spectra measured in D_2O. Chemical shifts and coupling constants were obtained from a first-order analysis of the spectra. All assignments were confirmed with the aid of two-dimensional $^{1}H/^{1}H$ COSY, $^{1}H/^{13}C$ HMQC, and ^{1}H NOESY experiments, using standard Bruker pulse programs. Processing of the spectra was performed with standard UXNMR (Bruker) and WIN-NMR software. Zero filling of the acquired data (512 t_1 values and 2K data points in t_2) led to a final data matrix of $1K \times 1K$ ($F_1 \times F_2$) data points. Analytical thin-layer chromatography (TLC) was performed on aluminum plates precoated with Merck silica gel 60F-254 as the adsorbent. The developed plates were air-dried, exposed to UV light and/or sprayed with a

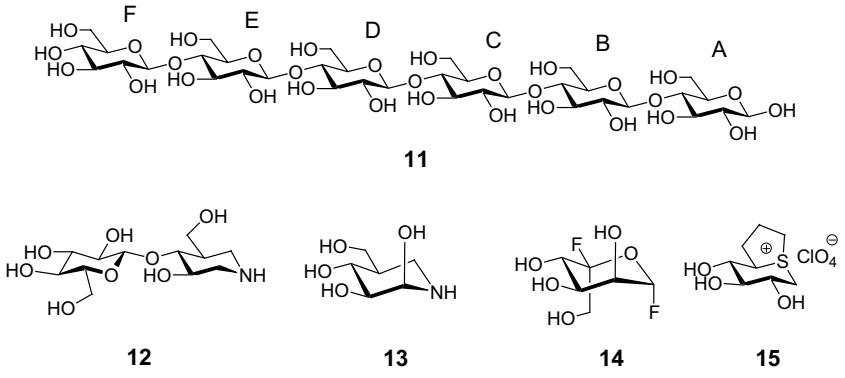

Chart 3.

solution containing 1% $Ce(SO_4)_2$ and 1.5% molybdic acid in 10% aqueous H_2SO_4 and heated. Compounds were purified by flash chromatography on Kieselgel 60 (230–400 mesh). Solvents were distilled before use and dried, as necessary, by literature procedures. Solvents were evaporated under reduced pressure and below 50 °C. High-resolution mass spectra were liquid secondary ionization fast atom bombardment (LSIMS(FAB)), using Cs^+ ions, run on a Kratos Concept H double focusing mass spectrometer at 10,000 RP, using *meta*-NO_2-benzyl alcohol as matrix or, as in the case of compounds **2** and **4**, with glycerine as matrix and PEG-sulfate as the mass reference. For purification by HPLC, crude compounds **2** and **4** were each dissolved in 1 mL water and applied to a medium-pressure ODS column. Compound **2** was eluted with water (5 mL/min) and compound **4** was eluted with (9:1) a water–acetonitrile mixture (4 mL/min). The fractions were collected and freeze-dried to give the desired products as white foams.

4.2. Synthesis

4.2.1. 5-Thio-D-glucopyranosylamine 3. 5-Thio-D-glucose **7** (0.1 g, 0.5 mmol) was dissolved in dry methanol (2 mL), the reaction mixture saturated with ammonia gas and was stirred for 4 days. TLC showed the formation of a more polar compound. The compound was isolated and purified using flash chromatography (EtOAc–MeOH–H_2O 6:4:1). The desired product **3** was obtained as a yellowish foam of an α:β (1:2) mixture (0.016 g, 16%). The starting material (0.077 g, 78%) was then recovered. Compound **3**: ^{1}H NMR (D_2O), minor α-anomer: δ 4.32 (d, 1H, $J_{1,2}$ = 4.3 Hz, H-1), 3.88 (m, 1H, H-2), 3.62–3.51 (m, 4H, H-3, H-4, H-6A, H-B), 3.20 (ddd, 1H, $J_{5,6A}$ = 3.8 Hz, $J_{5,6B}$ = 5.2 Hz, $J_{5,4}$ = 9.1 Hz, H-5). Major β-anomer: δ 4.00 (d, 1H, $J_{1,2}$ = 9.6 Hz, H-1), 3.91 (dd, 1H, $J_{6A,5}$ = 3.2 Hz, $J_{6A,6B}$ = 11.9 Hz, H-6A), 3.81 (dd, 1H, $J_{6B,5}$ = 6.1 Hz, H-6B), 3.55 (dd, 1H, $J_{4,3}$ = 9.1 Hz, H-4), 3.40 (t, 1H, $J_{2,3}$ = 9.4 Hz, H-2), 3.27 (t, 1H, $J_{3,4}$ = 9.1 Hz, H-3), 3.01 (ddd, 1H, $J_{5,4}$ = 9.4 Hz, H-5). ^{13}C NMR, minor α-anomer: δ 80.05 (C-2), 61.14 (C-3), 65.58 (C-6), 57.63 (C-1), 45.38 (C-5). Major β-anomer: δ 80.53 (C-2), 79.92 (C-3), 75.93 (C-4), 62.90 (C-6), 58.67 (C-1), 49.07 (C-5). Anal. Calcd for $C_6H_{13}S_1N_1O_4$: C, 36.91; H, 6.71; N, 7.17. Found: C, 36.60; H, 6.94; N, 6.84.

4.2.2. Improved synthesis of 5-thio-D-glucopyranosylamine 3. Compound **7** (0.9 g, 4.6 mmol) was dissolved in concentrated aqueous ammonia (50 mL) and the mixture stirred at room temperature for 3 days. Completion of reaction was tested using thin-layer chromatography. Evaporation of aqueous ammonia yielded the desired product, which was purified using column chromatography (EtOAc–MeOH–H_2O 6:3:1). Compound **3**, a yellowish foam, was obtained as an α:β (1:2) mixture (0.64 g, 71%).

4.2.3. 2-Phenylthioacetimidic acid phenyl ester hydrobromide 5.[12] Benzyl cyanide (5 mL, 43 mmol) was added to thiophenol (4.5 mL, 43 mmol) in diethyl ether (6 mL). The reaction mixture was stirred for 40 min, at 0 °C under an atmosphere of HBr. The white precipitate formed was then removed by filtration and rinsed with diethyl ether. Crude compound **5** was recrystallized from a mixture of acetonitrile and diethyl ether to give the desired product as white crystals (11.35 g, 85%). Mp 159 °C (dec). ^{1}H NMR ($CDCl_3$): δ 13.6 (s, 1H, NH_1), 9.5 (s, 1H, NH_2), 7.7–7.2 (m, 10H, 2Ph), 4.5 (s, 2H, CH_2Ph). ^{13}C NMR ($CDCl_3$): δ 196.23 (–C=N–), 135.33, 133.39, 131.82, 131.60, 129.90, 129.31, 128.76, 120.91 (C–2Ph), 42.03 (*C*H_2Ph). Anal. Calcd for $C_{14}H_{14}SNBr$: C, 54.55; H, 4.58; N, 4.54. Found: C, 54.37; H, 4.54; N, 4.66. MALDI-MS: Calcd for $C_{14}H_{14}SNBr$: 228.08 (M+Br); Found: 228.15 (M+Br).

4.2.4. 5-Thio-D-glucopyranosylamidinium bromide 4. Glucosylamine **3** (0.50 g, 2.6 mmol) was dissolved in dry pyridine, the thioimidate salt **5** (0.79 g, 2.6 mmol) then added, and the reaction mixture was stirred for 4 days at room temperature, under nitrogen. Completion of the reaction was indicated by TLC. The solvent was removed under reduced pressure and the compound purified by flash chromatography (EtOAc–MeOH–H_2O 7:3:1). The desired product was obtained as an α:β (1:7) mixture (0.35 g, 35%). The product was further purified using high performance liquid chromatography using water as the mobile phase. Pure compound **4** was obtained as an α:β (1:15) mixture (0.1 g, 10%). ^{1}H NMR (D_2O) Minor α-anomer: δ 7.49–7.26 (m, 5H, Ph), 4.90 (d, 1H, $J_{1,2}$ = 4.4 Hz, H-1), 4.04 (dd, 1H, $J_{2,3}$ = 9.7 Hz, H-2), 3.96 (s, 2H, CH_2Ph), 3.78 (dd, 1H, H-6A), 3.79 (dd, 1H, $J_{5,6B}$ = 3.2 Hz, $J_{6A,6B}$ = 11.9 Hz, H-6B), 3.65 (t, 1H, $J_{3,4}$ = 7.9 Hz, H-3), 3.63 (t, 1H, H-4), 2.88 (ddd, 1H, $J_{5,6A}$ = 5.3 Hz, $J_{5,4}$ = 8.4 Hz, H-5). Major β-anomer: δ 7.49–7.26 (m, 5H, Ph), 4.75 (d, 1H, $J_{1,2}$ = 9.3 Hz, H-1), 3.91 (dd, 1H, $J_{6A,5}$ = 3.2 Hz, $J_{6A,6B}$ = 12 Hz, H-6A), 3.90 (s, 2H, CH_2Ph), 3.83 (dd, 1H, $J_{6B,5}$ = 5.8 Hz, H-6B), 3.72 (t, 1H, $J_{2,3}$ = 9.3 Hz, H-2), 3.59 (dd, 1H, $J_{3,4}$ = 9.3 Hz, $J_{4,5}$ = 10.4 Hz, H-4), 3.30 (t, 1H, H-3), 3.05 (ddd, 1H, H-5). ^{13}C NMR (D_2O): δ 170.34 (–C=N), 131.98, 131.45, 130.98, (6C, Ph), 79.82 (C-3), 77.57 (C-2), 75.25 (C-4), 62.49 (C-6), 57.80 (C-1), 49.33 (C-5), 41.18 (*C*H_2Ph). HRMS Calcd for $C_{14}H_{21}N_2SBrO_4$ (M+Br): 313.1222. Found: 313.1225.

4.2.5. 5-Thio-D-mannose 6. 1,2,3,4,6-Penta-*O*-acetyl-5-thio-α-D-mannopyranose (1.0 g, 2.5 mmol) was dissolved in dry methanol. A catalytic amount of sodium methoxide was added and the reaction mixture stirred at room temperature for 1.5 h. The reaction mixture was neutralized using Rexyn 101 acid resin. The resin was removed by filtration and the desired product purified using column chromatography (EtOAc–MeOH–H_2O 7:3:1). Evaporation of the solvent gave an α:β (9:1) mixture of 5-thio-D-mannopyranose **2** as a white foam (0.37 g, 77%). ^{1}H NMR (D_2O) Major α-anomer: δ 4.88 (d, 1H, $J_{1,2}$ = 3.9 Hz, H-1), 4.14 (dd, 1H, $J_{2,3}$ = 2.6 Hz, H-2), 3.90 (dd, 1H, $J_{6A,5}$ = 3.4 Hz, $J_{6A,6B}$ = 11.9 Hz, H-6A), 3.80 (dd, 1H, $J_{6A,5}$ = 6.7 Hz, H-6B), 3.72–3.78 (m, 2H, H-3 and H-4), 3.19 (ddd, 1H, $J_{5,4}$ = 9.8 Hz, H-5). Minor β-anomer: δ 5.15 (d, 1H, $J_{1,2}$ = 1.9 Hz, H-1), 4.17 (dd, 1H, $J_{2,3}$ = 2.7 Hz, H-

2), 3.94 (dd, 1H, $J_{6A,5}$ = 3.5 Hz, $J_{6A,6B}$ = 11.8 Hz, H-6A), 3.78–3.70 (m, 2H, H-6B & H-4), 3.45 (dd, 1H, $J_{3,4}$ = 9.5 Hz, H-3), 2.95 (ddd, 1H, H-5). ^{13}C NMR (D_2O) Major α-anomer: δ 78.44 (C-1), 75.28 (C-2), 74.01 (C-3), 72.23 (C-4), 63.15 (C-6), 46.49 (C-5). Minor β-anomer: δ 76.60 (C-1), 76.42 (C-3), 63.34 (C-6), 48.32 (C-5).

4.2.6. 5-Thio-D-mannopyranosylamine 1. 5-Thio-D-mannose **6** (1 g, 5.1 mmol) was dissolved in aqueous ammonia (60 mL) and stirred at room temperature for 2 days. Completion of the reaction was tested using thin-layer chromatography. Evaporation of the aqueous ammonia yielded the desired product, which was purified using flash chromatography (EtOAc–MeOH–H_2O 6:3:1). Glycosylamine **1** was obtained as an α:β (1:3) mixture (0.79 g, 79%) in the form of a white foam. ^{1}H NMR (D_2O) Minor α-anomer: δ 4.07 (m, 1H, H-2), 3.92 (dd, 1H, H-6A), 3.78 (dd, 1H, $J_{6B,5}$ = 6.9 Hz, $J_{6A,6B}$ = 11.9 Hz, H-6B), 3.76 (t, 1H, $J_{4,3}$ = 9.6 Hz, H-4), 3.68 (m, 1H, H-3), 3.15 (ddd, 1H, $J_{5,4}$ = 11.0 Hz, $J_{5,6A}$ = 3.5 Hz, H-5). Major β-anomer: δ 4.35 (d, 1H, $J_{1,2}$ = 1.2 Hz, H-1), 4.06 (dd, 1H, H-2), 3.92 (dd, 1H, $J_{6A,6B}$ = 11.8 Hz, H-6A), 3.68 (dd, 1H, H-6B), 3.64 (t, 1H, $J_{4,3}$ = 9.4 Hz, H-4), 3.43 (dd, 1H, $J_{3,2}$ = 2.7 Hz, H-3), 2.96 (ddd, 1H, $J_{5,4}$ = 10.3 Hz, $J_{5,6A}$ = 3.3 Hz, $J_{5,6B}$ = 7.2 Hz, H-5). ^{13}C NMR (D_2O), Major β-anomer: δ 77.68 (C-3), 76.68 (C-2), 72.14 (C-4), 63.41 (C-6), 58.61 (C-1), 49.29 (C-5). Anal. Calcd for $C_6H_{13}SNO_4$: C, 36.91; H, 6.71; N, 7.17. Found: C, 36.97; H, 6.91; N, 6.87.

4.2.7. 5-Thio-D-mannopyranosylamidinium bromide 2. Mannopyranosylamine **1** (0.42 g, 2.15 mmol) was dissolved in dry pyridine, the thioimidate salt **5** (0.3 g, 0.76 mmol) added and the reaction mixture stirred for 4 days at room temperature, under nitrogen. Completion of reaction was tested by TLC. The solvent was removed under reduced pressure and the compound purified by flash chromatography (EtOAc–MeOH–H_2O 7:3:1). The desired product was obtained as an α,β mixture in 37% yield. The product was further purified by high performance liquid chromatography using water as the mobile phase with a flow rate of 4 mL/min. Pure **2α** (0.057 g, 7%) and **2β** (0.13 g, 18%) were isolated as white foams. ^{1}H NMR (D_2O) Minor α-anomer: δ 7.30–7.50 (m, 5H, Ph), 4.31 (d, 1H, $J_{1,2}$ = 4.5 Hz, H-1), 4.27 (dd, $J_{2,3}$ = 3.1 Hz, 1H, H-2), 3.91 (s, 2H, CH_2Ph), 3.88 (t, 1H, $J_{4,5}$ = 9.1 Hz, H-4), 3.84 (dd, 1H, $J_{6A,6B}$ = 12.1 Hz, $J_{6A,5}$ = 4.1 Hz, H-6A), 3.79 (dd, 1H, $J_{6B,5}$ = 6.5 Hz, H-6B), 3.74 (dd, 1H, $J_{3,4}$ = 8.7 Hz, H-3), 2.90 (ddd, 1H, H-5). ^{13}C NMR (D_2O): δ 169.35 (–C=N), 130.93, 131.30, 132.00, 135.39 (6C, Ph), 74.32 (C-3), 72.83 (C-2), 71.73 (C-4), 63.07 (C-6), 59.16 (C-1), 48.74 (C-5), 41.02 (CH_2Ph). HRMS Calcd for $C_{14}H_{21}N_2SBrO_4$ (M+Br): 313.1222. Found: 313.1218 $[\alpha]_D^{20} = +161$ (*c* 0.0041 g, H_2O).

β-anomer: δ 7.30–7.50 (m, 5H, Ph), 5.03 (d, 1H, $J_{1,2}$ = 2.2 Hz, H-1), 4.26 (t, $J_{2,3}$ = 2.5 Hz, 1H, H-2), 3.85 (dd, 1H, $J_{6A,5}$ = 4.4 Hz, H-6A), 3.84 (t, 1H, H-4), 3.65 (dd, 1H, $J_{6A,6B}$ = 11.9 Hz, $J_{6B,5}$ = 7.2 Hz, H-6B), 3.56 (dd, 1H, $J_{3,4}$ = 8.6 Hz, H-3), 2.98 (ddd, 1H, $J_{5,4}$ = 8.8 Hz, H-5). ^{13}C NMR (D_2O): δ 169.4 (–C=N), 130.27, 131.60, 131.99 (6C, Ph), 83.79 (C-3), 73.18 (C-2), 69.92 (C-4), 68.75 (C-6), 67.30 (C-1), 51.23 (C-5), 36.61 (CH_2Ph). HRMS Calcd for $C_{14}H_{21}N_2SBrO_4$ (M+Br): 313.1222. Found: 313.1219.

4.3. Enzyme inhibition

4.3.1. Golgi α-mannosidase II. Inhibition of mannosidase activity for compounds **4** and **6** was carried out in microtiter plates in a final volume of 50 μL. Inhibitors were dissolved in water to a final concentration of 200 mM. The reaction mixture consisted of 25 μL of 10 mM *para*-nitrophenyl α mannoside (PNP-mannose), 10 μL of 200 mM buffer and 10 μL of water or inhibitor. The buffer used was MES pH 5.75. The reaction mixture was pre-warmed to 37 °C and 5 μL of mannosidase diluted in 10 mM Tris pH 8, 100 mM NaCl was added to initiate the reaction. The amount of enzyme added was that which was necessary to keep the reaction in the linear range. In the case of the GMII this was approximately 350 ng of protein for a 15-min reaction. At the endpoint, the reaction was stopped using 50 μL of 0.5 M sodium carbonate. The absorbance of the reaction was measured at 405 nm with 520 nm background corrections on a microtiter plate reader. The 100% activity was the activity of the enzyme in the absence of any inhibitor. Activity remaining was calculated as a percentage of this uninhibited activity and a value of 50% inhibition (IC_{50}) was taken from plots of remaining activity versus inhibitor concentration.

4.3.2. Glucoamylase G2. The glucoamylase G2 from *Aspergillus niger* was purified from a commercial enzyme (Novo Nordisk, Bagsvaerd, Denmark) as described.[14,15] The initial rates of glucoamylase G2-catalyzed hydrolysis of maltose was tested with 1 mM maltose as substrate in 0.1 M sodium acetate pH 4.5 at 45 °C using an enzyme concentration of 7.0×10^{-8} M and five inhibitor concentrations in the range 1 μm–5 mM. The effect of the inhibition on rates of substrate hydrolysis for compounds **3** and **5**, were compared. The glucose released was analyzed in aliquots removed at appropriate time intervals using a glucose oxidase assay adapted to microtiter plate reading and using a total reaction volume for the enzyme reaction mixtures of 150 or 300 μL.[25] The K_i values were calculated assuming competitive inhibition from $1/V = (1/V_{max}) + [(K_M)/(V_{max}[S]K_i)] \times [I]$ (Fig. 37 and Fig. 38), where V is the rate measured in the presence or absence of inhibitor, [I] and [S] the concentrations of inhibitor and substrate, K_m 1.6 mM and k_{cat} 11.3 s^{-1}, using ENZFITTER.[26]

4.4. X-ray crystallography

4.4.1. Crystallization. Crystallization of *Drosophila* Golgi mannosidase II was carried out using hanging drop vapor diffusion as described previously.[7] In all cases, crystals were less than 24 h old at the time of crys-

tal evaluation and freezing. In the case of **1** and **2**, co-crystallization was successful in producing large well-diffracting crystals. Prior to freezing, the crystals were passed through drops containing 10%, 15%, 20%, and 25% 2-methyl-2,4-pentanediol. These cryo-solutions all contained 10 mM inhibitor. Inclusion of inhibitor in the cryo-solution was essential for visualizing clear electron density of these compounds. Subsequent to cryo-solution exposure, the crystals were mounted frozen in nylon CryoLoops (Hampton Research) directly in a liquid nitrogen cryostream.

4.4.2. Data collection. All data were collected at 100K. Data were collected at the Ontario Cancer Institute on a MAR Research 2300 image plate detector mounted on a rotating anode generator with Cu target, operated at 50 kV and 100 mA with beam focusing using Osmic optics. Typically, 300–400 frames of 0.5° oscillation were collected for each data set.

4.4.3. Refinement. The structures of the complexes were solved by molecular replacement starting with the unliganded enzyme structure (protein Data Bank code 1HTY).[3] Briefly, rigid body refinement was carried out against the published structure of native dGMII with Tris and waters in the region of the active site removed. This was followed by simulated annealing to 3500 K, group *B*-factor refinement and individual *B*-factor refinement, prior to generation of electron density maps.

Table 3. Statistics for data collection and refinement

Compound #	**1**	**2**
PDB code	**1R33**	**1R34**
HET symbol	LKA	LKS
Crystal		
Space group	$P2_12_12_1$	$P2_12_12_1$
Cell dimensions (Å)	68.84/109.91/138.89	68.77/109.56/138.74
Mosaicity	0.35	1.0
Data processing: overall (high resolution shell)		
Resolution (Å)	20–1.80 (1.86–1.80)	30–1.95 (2.02–1.95)
Reflections/redundancy	97070/7.1	73805/4.2
I/sigma	37.7 (7.1)	12.2 (3.14)
% Completeness	98.4 (84.5)	94.8 (95.0)
R merge	0.045 (0.178)	0.104 (0.378)
Refinement		
R_{test}/R_{free} (reflections for R_{free})	0.156/0.185 (2957)	0.151/0.196 (2143)
Amino acids	1014	1014
Water molecules	1153	1058
Rmsd bonds (Å)	1.80	1.90
Rmsd angles (°)	0.017	0.020
Average *B*-factor (Å^2)		
Overall	15.14	15.35
Protein main chain	12.67	12.78
Protein side chain	14.64	15.24
Water	25.40	24.86
Inhibitor	11.26	26.91
Zn	11.14	12.21
MPD	17.93	22.63
NAG	35.87	50.17

At this initial stage, *R*-factors were typically in the range of 22%, and the Fo–Fc density clearly showed the presence of bound compound and unassigned waters. Subsequent iterative rounds of refinement and visual fitting to the electron density resulted in the final statistics presented in Table 3. Final coordinates and diffraction data are deposited in the Protein Data Bank under codes 1R33 and 1R34. The intermolecular interactions were analyzed using Insight II software.

4.5. Molecular modeling

To investigate the interactions of ligands **3** and **4** with glucoamylase, the protonated forms of compounds **3** and **4** were docked into the active site in various conformations using AutoDock 3.0.[27] The structures were built using Sybyl 6.6 molecular modeling software (Tripos, Inc.). The structure energy minimization was performed using the standard Tripos molecular mechanics force field and Gasteiger–Marsili charges,[28] with a 0.001 kcal/mol energy gradient convergence criterion. The six-membered ring of compounds **3** and **4** was constructed in the following different conformations: 2 chair conformations ($^4C_1$ and $^1C_4$); 6 boat conformations ($^{1,4}B$, $B_{1,4}$, $^{2,5}B$, $B_{2,5}$, $^{3,0}B$, $B_{3,0}$); 6 skew conformations ($^1S_3$, $^3S_1$, $^5S_1$, $^1S_5$, $^3S_5$, and $^5S_3$) and 1 half-chair conformation $^2H_3$. Thus, 15 starting conformations of each of **3** and **4** were obtained for the docking simulations.

The crystallographic coordinates of glucoamylase were extracted from the Protein Data Bank [(PDB entry 1DOG, X-ray structure of the complex of 1-deoxynojirimycin **9** with glucoamylase from *Aspergillus awamori* var. X100 at 2.4 Å[17] and were analyzed using the Sybyl 6.6 program (Tripos, Inc.)]. All water molecules were removed from the structure except the water 501. Only polar hydrogen atoms were added to the protein, and Kollman united-atom partial charges[29] were assigned. At the start of each docking simulation, the six-membered ring of each conformation of compound **3** and **4** was superimposed over the equivalent part of 1-deoxynojirimycin **9**, from the crystal structure of the glucoamylase complex.[17]

The grid maps representing protein were calculated using Autogrid version 3.0.[27] In all cases, we used grid maps with $60 \times 60 \times 60$ points, and a grid-point spacing of 0.375 Å. All the rotatable bonds in the ligand were allowed to rotate. For **3**, 100 simulations were performed and for **4**, 300 simulations were performed. A Lamarckian Genetic Algorithm (LGA) was used to search for potential binding modes. For the analysis of the docked conformations, the clustering tolerance for the root-mean-square positional deviation was 2 Å with respect to the starting position.

The energies of the docked complexes of **3** and **4** in the glucoamylase active site in different conformations are shown in Table 4. The lowest-energy binding mode for each of protonated **3** and protonated **4** was the $^2H_3$ half-chair conformation.

Table 4. Docking results for compounds **3** and **4** in the glucoamylase active site.[a]

Conformation of six-membered ring	Final docked energy (kcal/mol)	
	Compound **3**	Compound **4**
$^{2}H_{3}$	−7.41(−7.28)	−11.19(−10.78)
$^{1}C_{4}$	−5.91(−5.61)	−9.28(−8.27)
$^{4}C_{1}$	−7.10(−6.97)	−10.47(−9.79)
$^{1,4}B$	−6.84(−6.66)	−9.44(−8.44)
$B_{1,4}$	−6.41(−6.00)	−9.80(−8.73)
$^{2,5}B$	−6.14(−5.74)	−10.24(−8.79)
$B_{2,5}$	−6.21(−5.99)	−9.33(−8.07)
$^{3,0}B$	−6.75(−6.51)	0.9(1.72)
$B_{3,0}$	−6.40(−6.28)	−9.29(−8.17)
$^{1}S_{3}$	−6.82(−6.56)	−10.30(−7.98)
$^{3}S_{1}$	−6.28(−5.96)	−9.70(−8.79)
$^{5}S_{1}$	−5.88(−5.57)	−9.16(−7.92)
$^{1}S_{5}$	−6.26(−5.92)	−9.86(−8.45)
$^{3}S_{5}$	−6.96(−6.66)	−10.37(−9.24)
$^{5}S_{3}$	−6.28(−5.91)	−9.79(−8.78)

[a] Docked structures are grouped into clusters, the best clusters being shown. The energy of the optimal structure in each cluster is to the left and that of the cluster average is given in parentheses.

Acknowledgements

We are grateful to the Natural Sciences and Engineering Research Council of Canada and the Canadian Institutes of Health Research for financial support. We also thank Sidsel Ehlers for technical assistance.

References

1. *Essentials of Glycobiology*; Varki, A., Cummings, R., Esko, J., Freeze, H., Hart, G., Marth, J., Eds.; Cold Spring Harbor Laboratory: Cold Spring Harbor, NY, 1999; Taylor, M. E.; Drickamer, K. *Introduction to Glycobiology*; Oxford University Press: New York, NY, 2003.
2. Herscovics, A. Carbohydrates and their derivatives including tannins, cellulose and related lignans. In *Comprehensive Natural Products Chemistry*; Pinto, B. M., Ed.; Barton, D. H. R., Nakanishi, K., Meth-Cohn, O., Eds.; Elsevier: UK, 1999; Vol. 3, Chapter 2.
3. Lillelund, V. H.; Jensen, H. H.; Liang, X.; Bols, M. *Chem. Rev.* **2002**, *102*, 515–553, and references cited therein.
4. Andrews, J. S.; Weimar, T.; Frandsen, T. P.; Svensson, B.; Pinto, B. M. *J. Am. Chem. Soc.* **1995**, *117*, 10799–10804.
5. Eldin, S.; Digits, J. A.; Huang, S.-T.; Jencks, W. P. *J. Am. Chem. Soc.* **1995**, *117*, 6631–6632.
6. Guo, W.; Hiratake, J.; Ogawa, K.; Yamamoto, M.; Ma, S. J.; Sakata, K. *Bioorg. Med. Chem. Lett.* **2001**, *11*, 467–470.
7. Inoue, K.; Hiratake, J.; Mizutani, M.; Takada, M.; Yamamoto, M.; Sakata, K. *Carbohydr. Res.* **2003**, *338*, 1477–1490.
8. Goss, P. E.; Baker, M. A.; Carver, J. P.; Dennis, J. W. *Clin. Cancer Res.* **1995**, *1*, 935–944.
9. van den Elsen, J. M. H.; Kuntz, D. A.; Rose, D. R. *EMBO J.* **2001**, *20*, 3008–3017.
10. Weill, C. E.; Bursch, R. J.; Van Dyk, J. W. *Cereal Chem.* **1954**, *31*, 150–158.
11. Driguez, H.; Henrissat, B. *Tetrahedron Lett.* **1981**, *22*, 5061–5062.
12. Yuasa, H.; Izukawa, Y.; Hashimoto, H. *J. Carbohydr. Chem.* **1989**, *8*, 753–763.
13. Baati, R.; Gouvernuer, V.; Mioskowski, T. *Synthesis* **1999**, *6*, 927–929.
14. Svensson, B.; Pedersen, T.; Svendsen, I.; Sakai, T.; Ottesen, M. *Carlsberg Res. Commun.* **1982**, *47*, 55–69.
15. Stoffer, B.; Frandsen, T. P.; Busk, P. K.; Schneider, P.; Svendsen, I.; Svensson, B. *Biochem. J.* **1993**, *292*, 197–202.
16. Kuntz, D. A.; Ghavami, A.; Johnston, B. D.; Pinto, B. M.; Rose, D. R. *Tetrahedron: Asymmetry* **2005**, *16*, 25–32.
17. Harris, E. M. S.; Aleshin, A. E.; Firsov, L. M.; Honzatko, R. B. *Biochemistry* **1993**, *32*, 1618–1626.
18. Aleshin, A. E.; Stoffer, B.; Firsov, L. M.; Svensson, B.; Honzatko, R. B. *Biochemistry* **1996**, *35*, 8319–8328.
19. Lorthiois, E.; Meyyappan, M.; Vasella, A. *J. Chem. Soc., Chem. Commun.* **2000**, *22*, 1829–1830.
20. Guerin, D. M. A.; Lascombe, M.-B.; Costabel, M.; Souchon, H.; Lamzin, V.; Beguin, P.; Alzari, P. M. *J. Mol. Biol.* **2002**, *316*, 1061–1069.
21. Varrot, A.; MacDonald, J.; Stick, R. V.; Gavin, P.; Gilbert, H. J.; Davies, G. J. *J. Chem. Soc., Chem. Commun.* **2003**, 946–947.
22. Kuntz, D. A.; Rose, D. R., unpublished observations.
23. Numao, S.; Kuntz, D. A.; Withers, S. G.; Rose, D. R. *J. Biol. Chem.* **2003**, *278*, 48074–48083.
24. Johnson, M. A.; Jensen, M. T.; Svensson, B.; Pinto, B. M. *J. Am. Chem. Soc.* **2003**, *125*, 5663–5670.
25. Frandsen, T. P.; Dupont, C.; Lehmbeck, J.; Stoffer, B.; Sierks, M. R.; Honzatko, R. B.; Svensson, B. *Biochemistry* **1994**, *33*, 13808–13816.
26. Leatherbarrow, R. J. *Enzfitter, a Nonlinear Regression Data Analysis Programme for IBM PC*; Elsevier Science: Amsterdam, The Netherlands, 1987.
27. Morris, G. M.; Goodsell, D. S.; Halliday, R. S.; Huey, R.; Hart, W. E.; Belew, R. K.; Olson, A. J. *J. Comput. Chem.* **1998**, *19*, 1639–1662.
28. Gasteiger, J.; Marsili, M. *Org. Magn. Reson.* **1981**, *15*, 353–360.
29. Cornell, W. D.; Cieplak, P.; Bayly, C. I.; Gould, I. R.; Merz, K. M., Jr.; Ferguson, D. M.; Spellmeyer, D. C.; Fox, T.; Caldwell, J. W.; Kollman, P. A. *J. Am. Chem. Soc.* **1995**, *117*, 5179–5197.
30. DeLano, W. L. *The PyMol Molecular Graphics System*; DeLano Scientific: San Carlos, CA, USA, 2002.
31. Kraulis, P. J. *J. Appl. Cryst.* **1991**, *24*, 946–950.